Science Advances
AAAS

Supplementary Materials for

Surficial nano-deposition locoregionally yielding bactericidal super CAR-macrophages expedites periprosthetic osseointegration

Ziyang Li *et al.*

Corresponding author: Xinyi Jiang, xinyijiang@sdu.edu.cn; Wei Li, wl80sph@163.com

Sci. Adv. **9**, eadg3365 (2023)
DOI: 10.1126/sciadv.adg3365

The PDF file includes:

Other Supplementary Material for this manuscript includes the following:

Supporting Figures

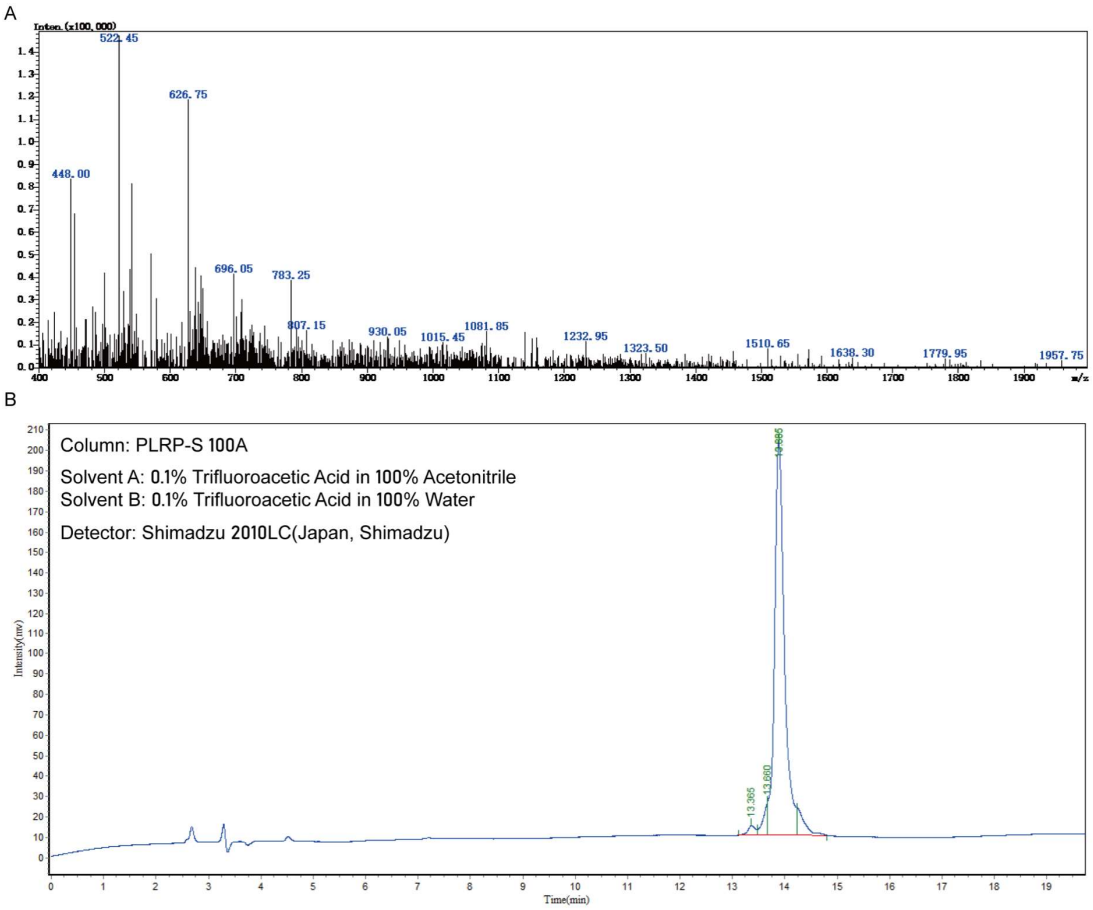

Figure S1. Characterization of the amphiphilic peptide-SA monomer. (A) The molecular weight of the peptide-SA monomer was certified by electrospray ionization mass spectrometry (ESI-MS). (B) The purity of the peptide was confirmed by high-performance liquid chromatography (HPLC).

A

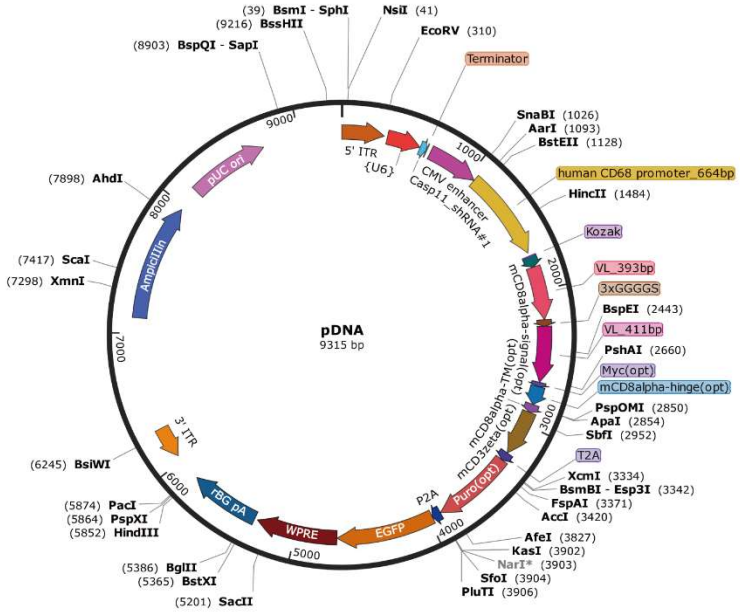

B

Figure S2. Diagram of the pDNA plasmid construction with a CD68 promoter. (A) Map of the pDNA plasmid. (B) Representative sequencing result of the CD68 promoter in the pDNA plasmid.

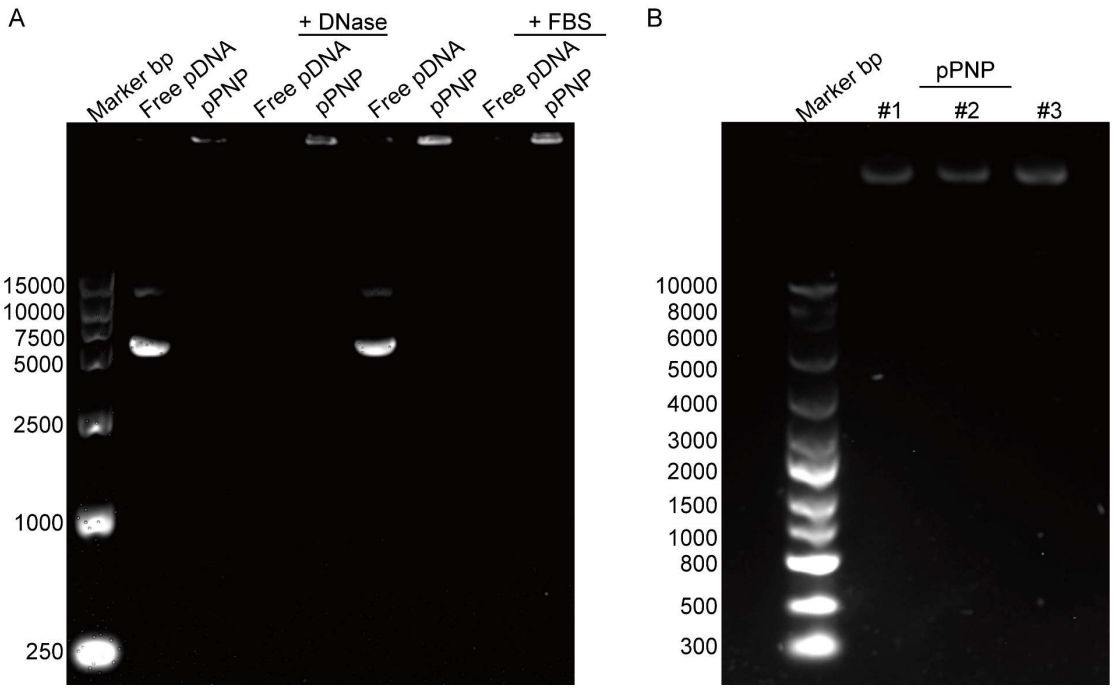

Figure S3. Gel retardation assay of pPNP. (A) The stability of pPNP when the weight ratio of peptide-SA monomers to the pDNA was 10:1. (B) Gel retardation assay the stability of pPNP after 14 days. The experiments were repeated three times independently. DNase I digestion and fetal bovine serum (FBS) treatment were performed at 37 °C for 1 h.

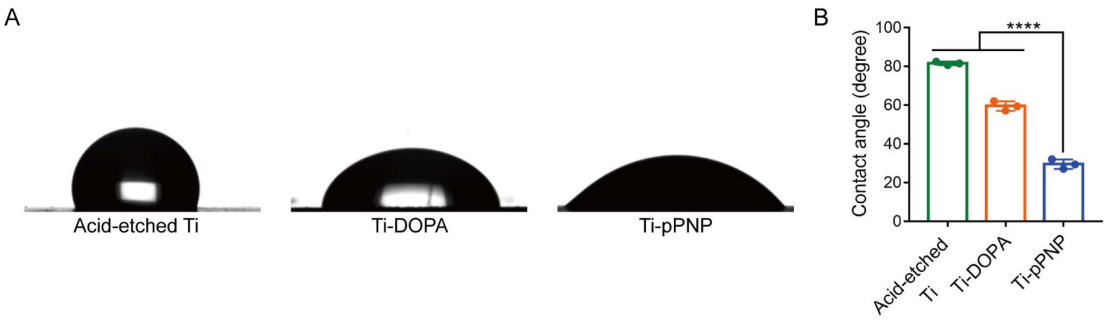

Figure S4. Water contact angle (WCA) of Control, Ti-DOPA, and Ti-pPNP. Data are presented as the mean ± SD. $n = 3$ independent experiments per group, ****$p < 0.0001$.

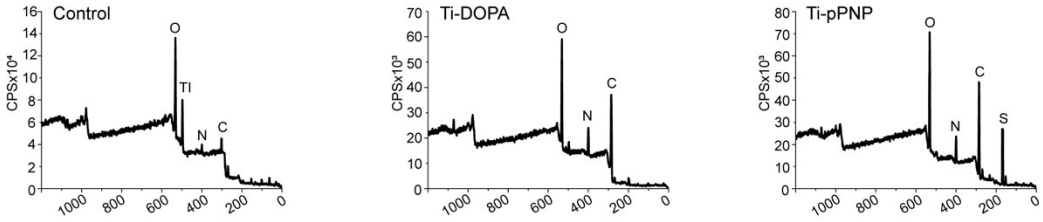

Figure S5. X-ray photoelectron spectroscopy (XPS) of Control, Ti-DOPA, and Ti-pPNP. *n* = 3 independent experiments per group.

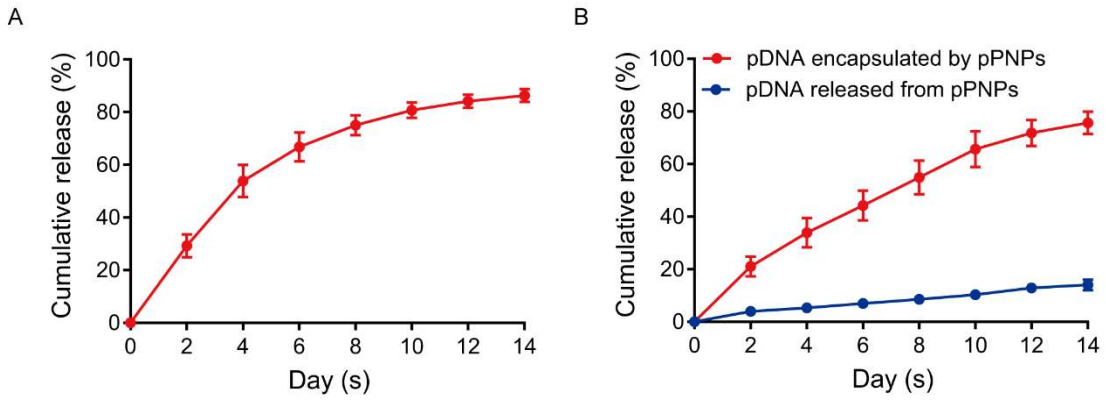

Figure S6. Relative release profile of HS and pPNP in vitro. (A) The release profile of HS from the coating. (B) The release profile of free pDNA or pPNP. Data are presented as the mean ± SD. $n = 3$ independent experiments per group.

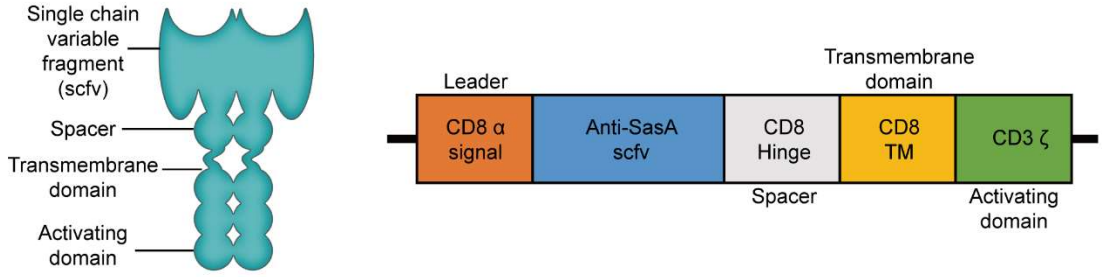

Figure S7. Diagram and sequence of a CAR incorporating a CD8 leader signal peptide, a SasA-targeting domain, a CD8 hinge, a CD8 transmembrane domain, and CD3 intracellular activating domains.

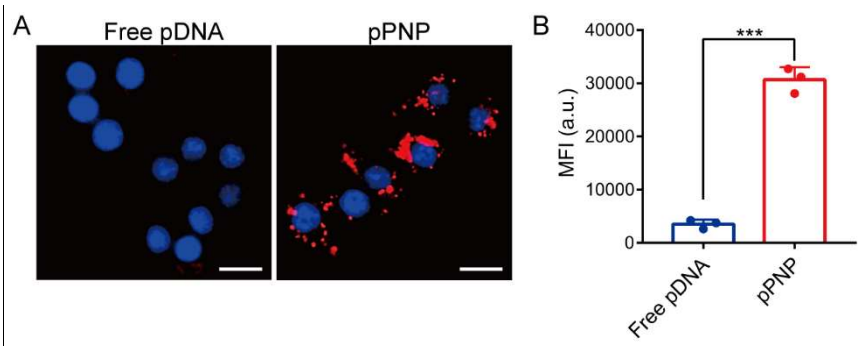

Figure S8. Cellular uptake of the pPNP by macrophages. (A) Confocal images of RAW 264.7 cells treated with free pDNA or pPNP. The nuclei were counterstained with DAPI (blue). Scale bar, 20 μm. (B) Cellular uptake of free pDNA or pPNP by RAW 264.7 cells as measured by flow cytometry analysis. Data are presented as the mean ± SD. $n = 3$ independent experiments per group, ***$p < 0.001$.

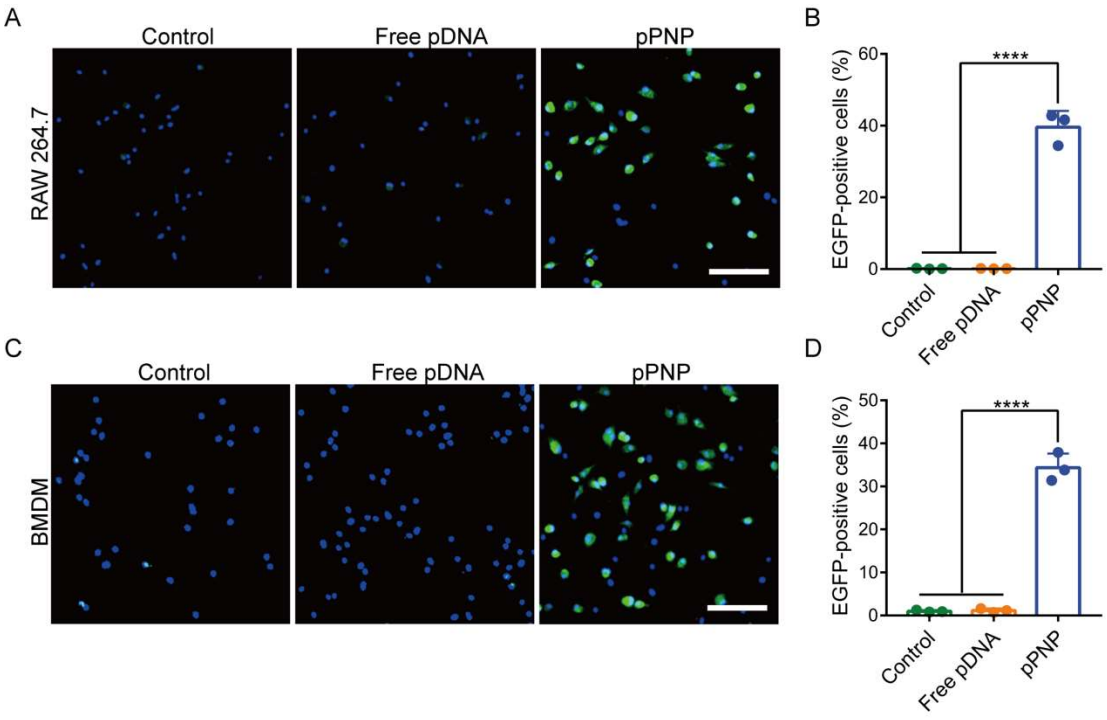

Figure S9. The percentage of EGFP-positive cells after different treatments. (A–D) Representative microscopy images (A, C) and quantitative analysis of the percentage (B, D) of EGFP-positive RAW 264.7 cells (A, B) or BMDMs (C, D) in the indicated groups after treatment. Scale bar: 100 μm. Data are presented as the mean ± SD. $n = 3$ independent experiments per group, ****$p < 0.0001$.

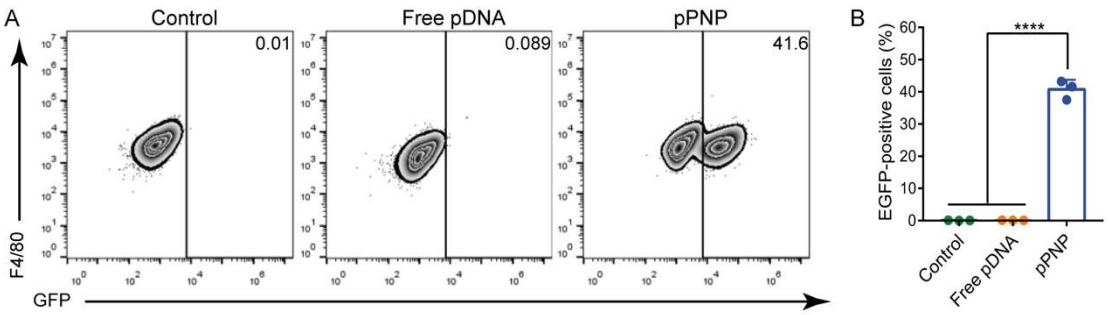

Figure S10. Percentage of EGFP-positive RAW 264.7 cells treated with free pDNA or pPNP. (A–B) Representative flow cytometry plots (A) and quantitative analysis (B) of the CAR expression in RAW 264.7 cells in the indicated treatment groups. Data are presented as the mean ± SD. $n = 3$ independent experiments per group, ****$p < 0.0001$.

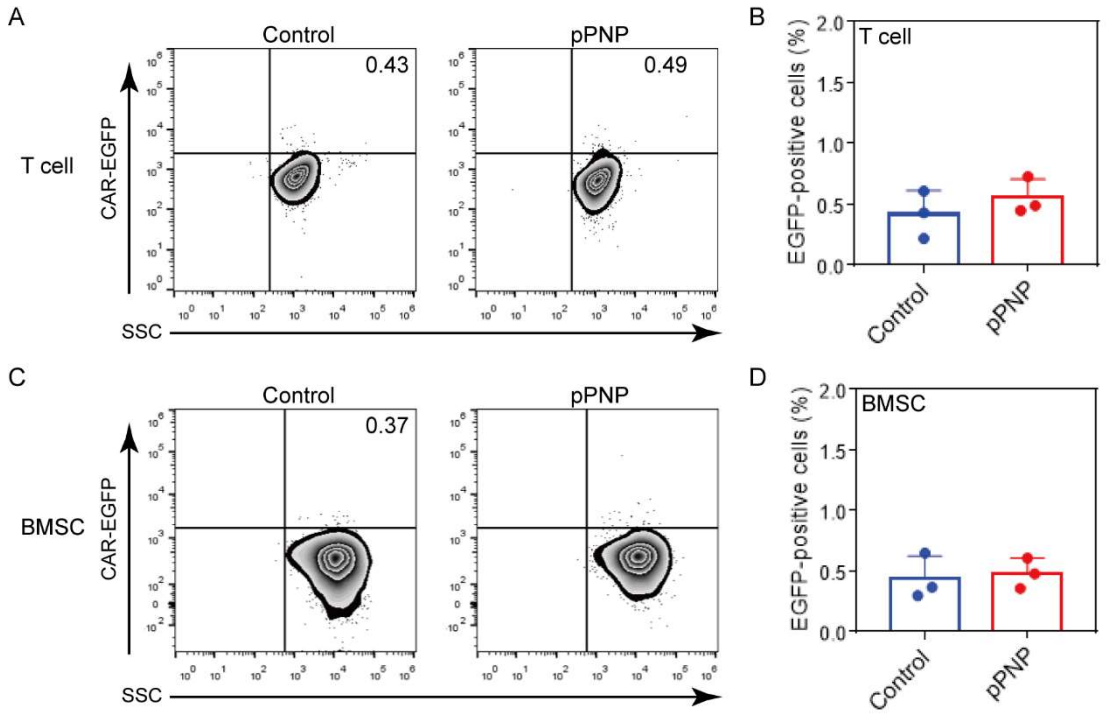

Figure S11. The CD68 promoter ensured macrophage-specific CAR transgene expression. (A–D) Mouse T cells and BMSCs were transduced with pDNA including the CD68 promoter. (A, C) The percentage of EGFP-positive T cells (A) or BMSCs (C) after treatment with control or pPNP. (B, D) Quantitative analysis of the flow cytometry data. Data are presented as the mean ± SD. n = 3 independent experiments per group.

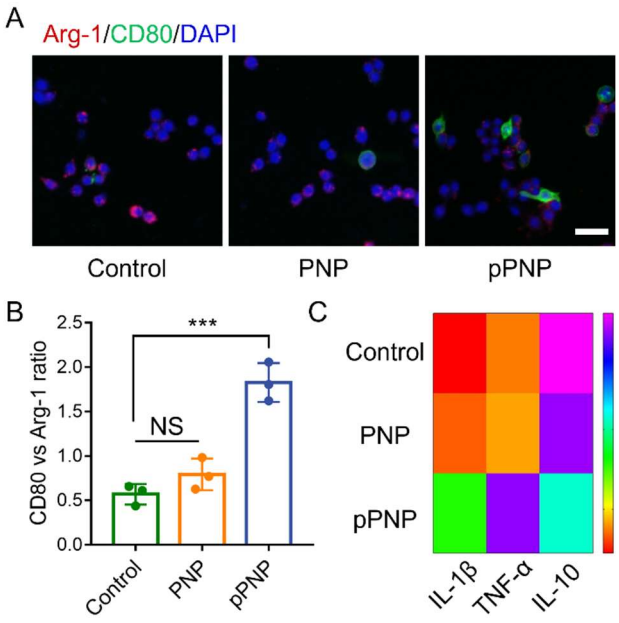

Figure S12. The phenotype of macrophages was changed after treatment with PBS, PNP, or pPNP. (A) Representative immunofluorescent staining of BMDMs that were treated with different groups. Scale bar: 50 μm. (B) Quantitative analysis of the relative fluorescence intensity of $CD80^+$ staining versus $Arg\text{-}1^+$ staining in each group. (C) Heatmap of the IL-1β, TNF-α, and IL-10 expression profiles in BMDMs treated with different groups. $n = 3$ independent experiments per group, ***$p < 0.001$, NS = not significant.

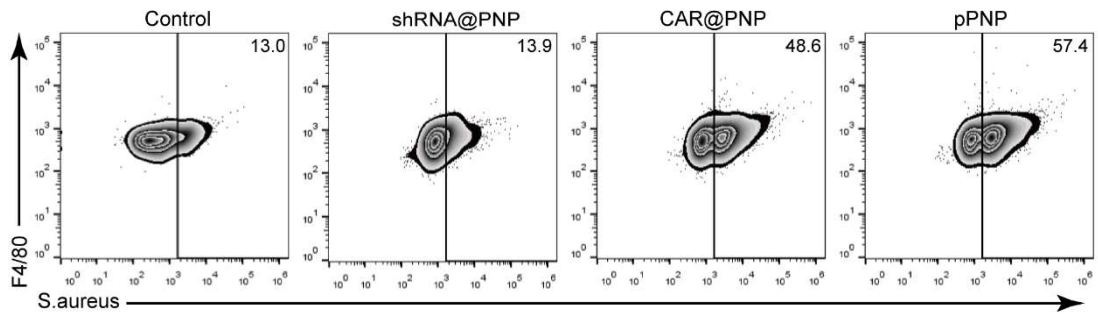

Figure S13. Representative flow cytometry plots of the phagocytosis of MRSA by macrophages treated with each formulation. $n = 3$ independent experiments per group.

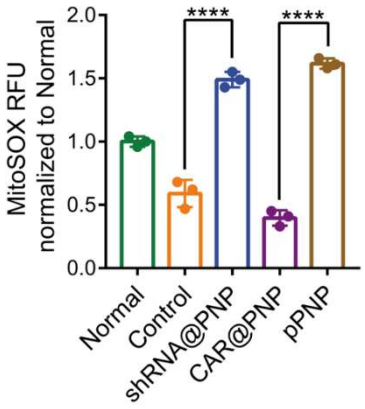

Figure S14. MitoSOX assay conducted on different treatment groups of BMDMs infected with MRSA (multiplicity of infection = 5:1) at 4 h post-infection. Data are presented as the mean ± SD. $n = 3$ independent experiments per group, ****$p < 0.0001$.

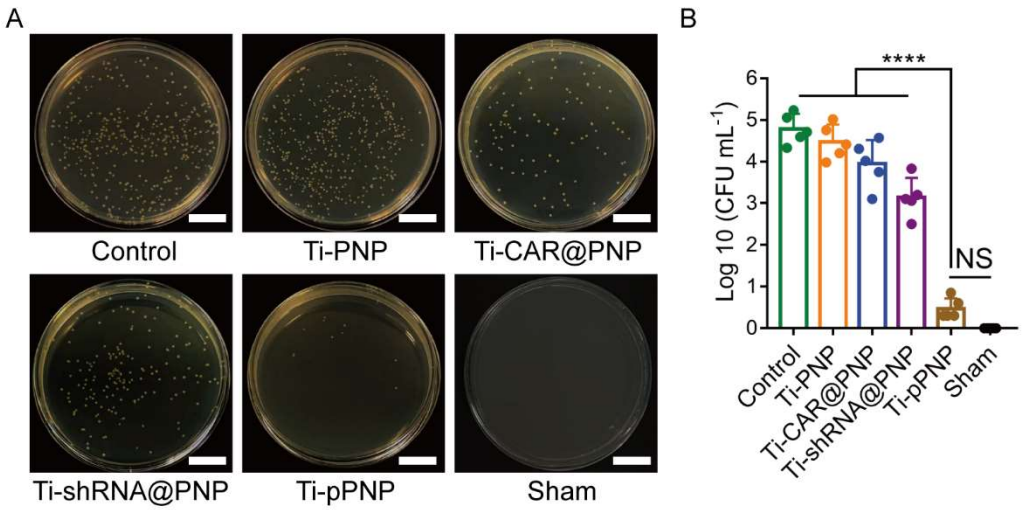

Figure S15. Quantified antibacterial efficiency. (A) Representative images of the bacterial colonies from the coated implants and surronding tissues harvested from the indicated treatment groups. (B) Quantified antibacterial efficiency of each treatment group. Data are presented as the mean ± SD. $n = 5$ independent experiments per group, ****$p < 0.0001$, NS = not significant.

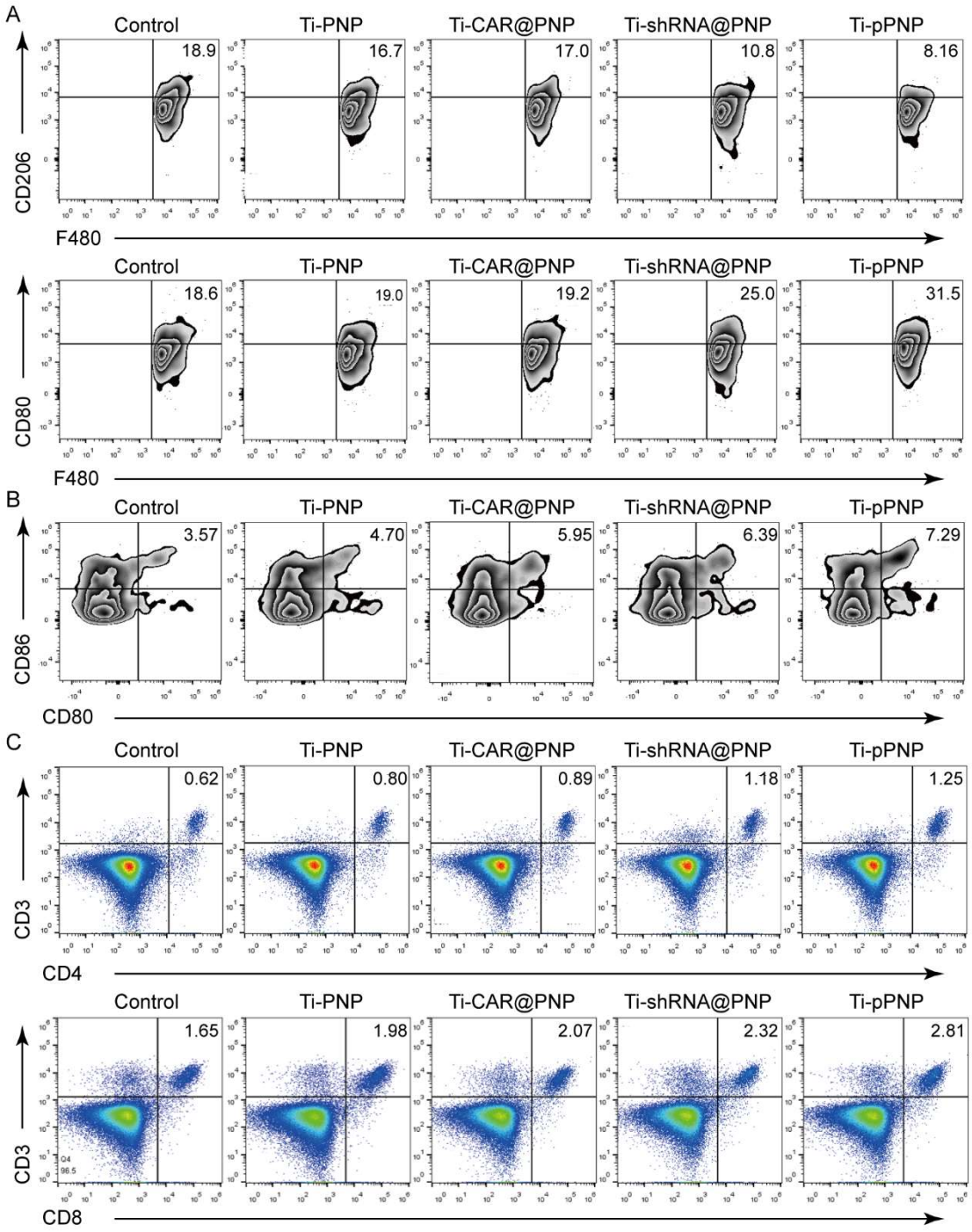

Figure S16. The immune cell landscape profile change in infection after various treatments. (A) Representative flow cytometry plots of M2-like macrophages and M1-like macrophages in the implant-associated tissues of mice from the indicated treatment groups (n = 5). (B) Representative flow cytometry plots of mature dendritic cells (DCs) in the draining lymph nodes (n = 5). (C) Representative flow cytometry plots of $CD4^+$ and $CD8^+$ T cells in the implant-associated tissues of mice from the indicated treatment groups (n = 5).

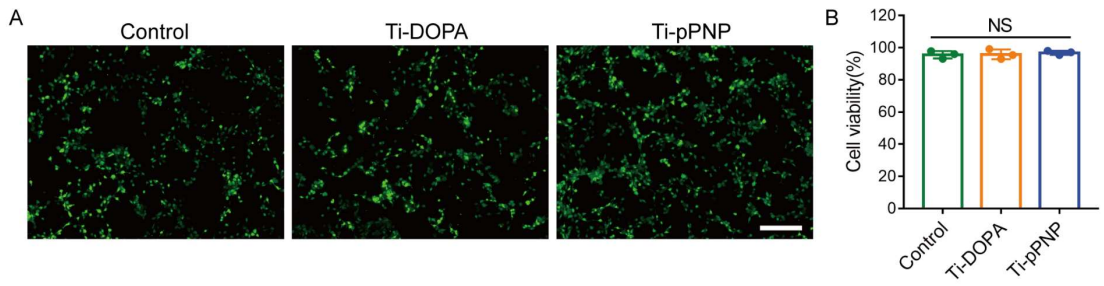

Figure S17. Biocompatibility evaluation of pPNP coating. (A) Representative fluorescence images of the proliferation of BMSCs cultured for 3 days on titanium plates with the indicated coating. Scale bar: 100 μm. (B) Cytotoxic effect of the titanium plate surficial coating on BMSCs, as measured by the standard methyl thiazolyl tetrazolium assay. Data are presented as the mean ± SD. n = 3 independent experiments per group, NS = not significant.

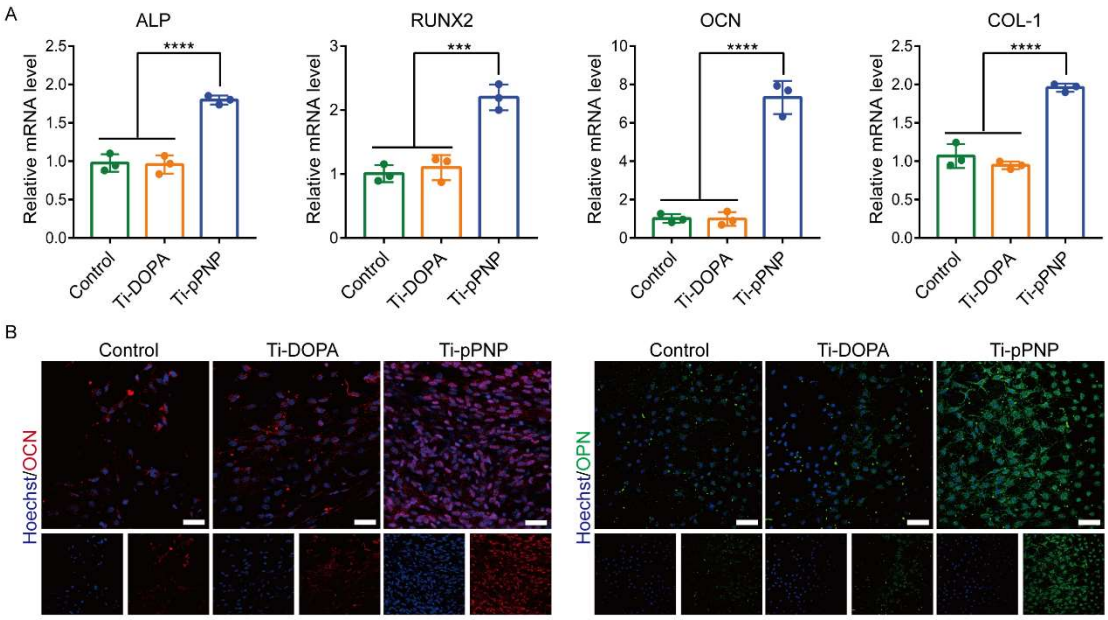

Figure S18. pPNP coating-induced osteogenesis in vitro. (A) The expression of the osteogenesis-related genes ALP, RUNX2, OCN, and COL-I in BMSCs that were cultured for 14 days on titanium plates with the indicated coating. (B) OCN (red: OCN; blue: nucleus) and OPN (green: OPN; blue: nucleus) staining of BMSCs cultured for 14 days on titanium plates with the indicated coating. Scale bar: 50 μm. Data are presented as the mean ± SD. $n = 3$ independent experiments per group, ***$p < 0.001$ and ****$p < 0.0001$.

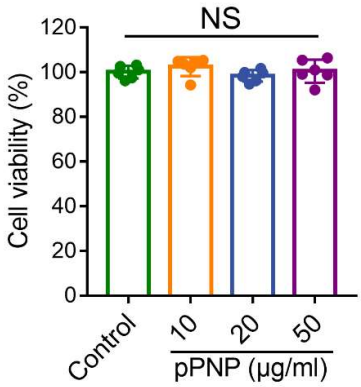

Fig. S19. Cytotoxicity of the pPNP toward macrophage. Data are presented as the mean ± SD. *n* = 6 independent experiments per group, NS = not significant.

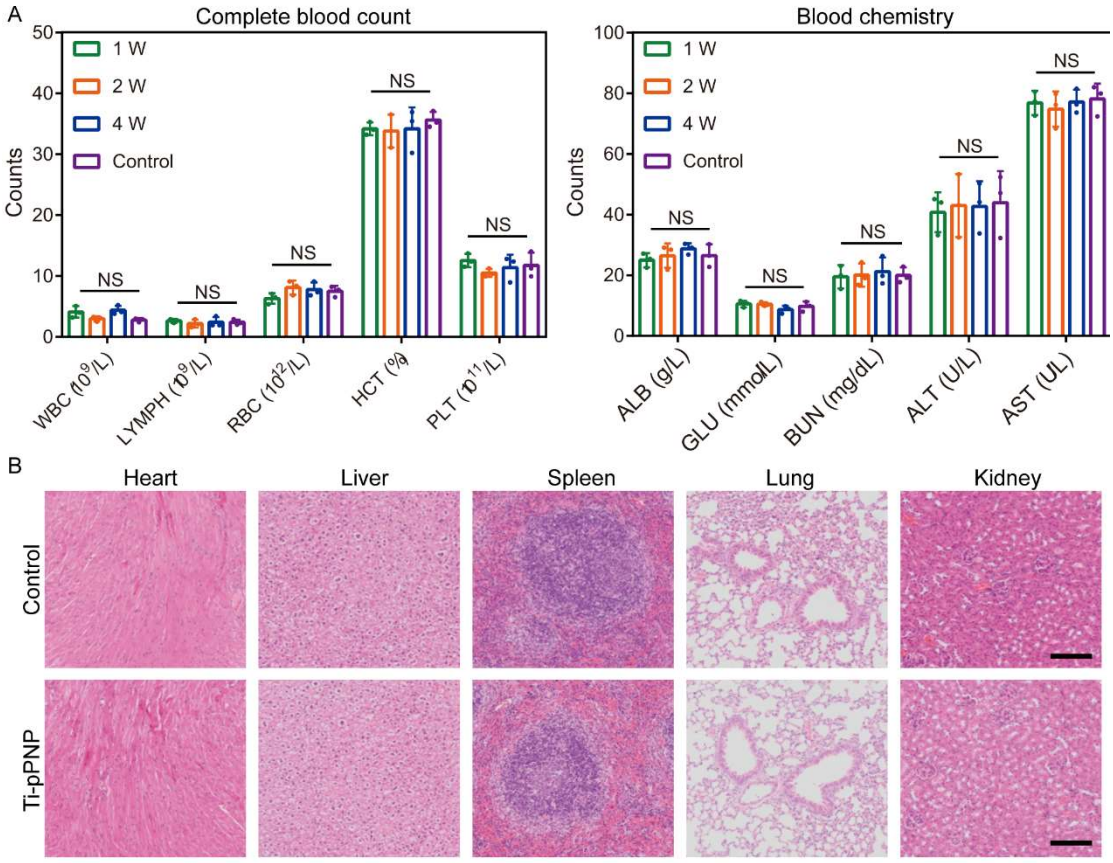

Figure S20. Systemic toxicity evaluation of the pPNP coating. (A) Complete blood count and blood chemistry of control (healthy animal without surgery) mice and mice with a Ti-pPNP implant at 1, 2, and 4 weeks after implantation. WBC, white blood cell; LYMPH, lymphocyte; RBC, red blood cell; HCT, hematocrit; PLT, platelet; ALB, albumin; GLU, glucose; BUN, blood urea nitrogen; ALT, alanine transaminase; AST, aspartate transaminase. (B) Histological analysis of the major organs from control (healthy animal without surgery) mice or mice with a Ti-pPNP implant. Scale bar: 500 μm. Data are presented as the mean ± SD. n = 3 independent experiments per group, NS = not significant.

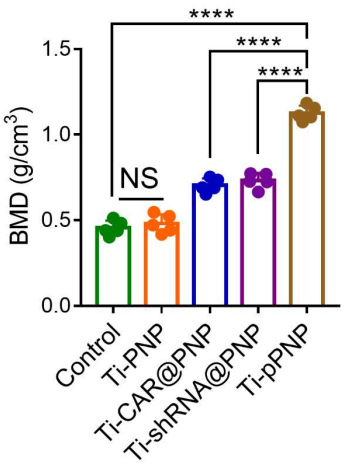

Figure S21. Quantified bone mineral density (BMD) based on micro-CT monitoring of different groups. Data are presented as the mean ± SD. $n = 5$ independent experiments per group, ****$p < 0.0001$, NS = not significant.

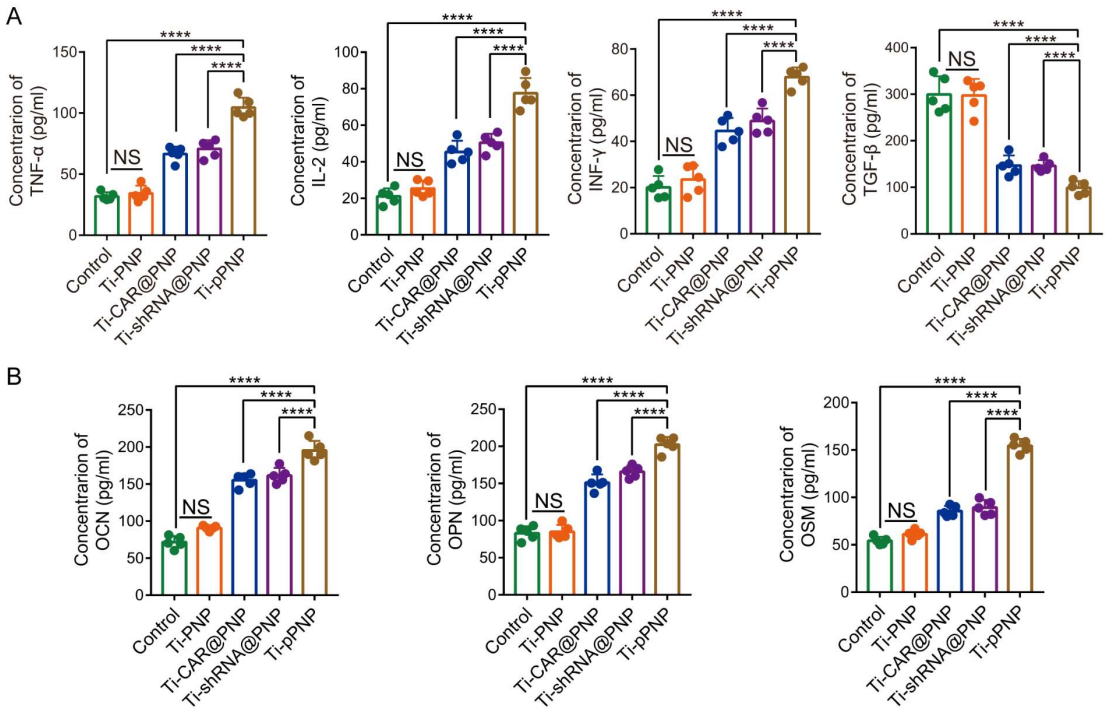

Figure S22. The extent of hematogenous implant infection evaluation after treated with different groups. (A) Concentrations of TNF-α, IL-2, IFN-γ and TGF-β in implant-associated tissue from mice receiving the indicated treatment. (B) Concentrations of OPN, OSM and OCN in implant-associated tissue from mice receiving the indicated treatment. n = 5 independent experiments per group, ****p < 0.0001, NS = not significant.

Supplementary Table 1. Sequences of the primers used in this study

Col-1	Forward	5’- GAGAGGTGAACAAGGTCCCG-3’
	Reverse	5’- AAACCTCTCTCGCCTCTTGC-3’
Runx2	Forward	5’- AGCGGACGAGGCAAGAGTTT-3’
	Reverse	5’- AGGCGGGACACCTACTCTCATA-3’
ALP	Forward	5'- TGAGCGACACGGACAAGAAG-3’
	Reverse	5'- CCTGGTAGTTGTTGTGAGCGTAAT-3’
OCN	Forward	5’- AAAGGCGACAAGGACGGC-3’
	Reverse	5’- AGAAGTAATCCAGCACCAGCCAT-3’
OPN	Forward	5’- TGGCTGAATTCTGAGGGACTAA-3’
	Reverse	5’- GCAGGCTGTAAAGCTTCTTCTCC-3’
β-actin	Forward	5'- GTGACGTTGACATCCGTAAAGA-3’
	Reverse	5'- GTAACAGTCCGCCTAGAAGCAC-3’

Source Data: dg3365_Suppl. Excel_seq1_v1.xlsx